

Study on the classification of chronic gastritis at molecular biological level

Goang-Yao Yin, Wu-Ning Zhang, Xue-Fen He, Yi Chen, Xiao-Jing Shen

Goang-Yao Yin, Xue-Fen He, Xiao-Jing Shen, Wuxi No.3 Peoples Hospital, Wuxi 214041, Jiangsu Province, China

Wu-Ning Zhang, Yi Chen, Department of National Microanalysis Center, Fudan University, Shanghai 200433, Shanghai, China

Correspondence to: Dr. Goang-Yao Yin, Wuxi No.3 Peoples Hospital, 230 Eastern Tonghuhui Road Wuxi 214041, Jiangsu Province, China. yinyao@pub.wx.jsinfo.net

Received: 2002-10-04 **Accepted:** 2002-12-03

Abstract

AIM: To explore the pathophysiological basis for the fact that patients with digestive tract symptoms do not necessarily have gastric mucosal pathology and those without clinical symptoms do not necessarily have no gastric mucosal pathology.

METHODS: The ultrastructure, trace elements, cAMP, DNA, SOD and LPO in the gastric mucosa and its epithelial cells of 188 patients without organic lesions of heart, lung, liver, gallbladder, pancreas, kidney or intestine and basically histopathological normal persons (F) were detected synchronously by SEM, TEM, EDAX, Image analysis system RIA and ³H-TdR Lymphocyte Transfer Test.

RESULTS: The content of Zn, Cu, cAMP and ³H-TdR LCT in gastric mucosa and the content of Zn, Cu, DNA and LPO in gastric mucosa epithelial nuclei of each group were shown as follows: Normal control (4.1±1.0, 5.2±0.8, 15.9±1.5, 1079.7±227.4, 7.6±0.4, 58.4±0.3, 12.6±2.7, 2.6±0.6); CSG without symptoms group (3.7±1.2, 5.1±1.8, 15.6±0.9, 924.5±234.9, 7.8±0.3, 58.6±0.4, 13.0±3.1, 2.9±0.4); CAG without symptoms group (3.3±1.0, 4.8±0.9, 14.9±0.7, 887.7±243.6, 7.8±0.3, 58.7±0.3, 14.3±2.8, 3.1±0.4); F type with symptoms group (3.5±1.4, 4.5±1.0, 15.7±1.4, 932.1±2449.3, 7.9±0.4, 58.7±0.5, 13.5±4.6, 2.9±0.7); CSG with symptoms group (2.8±1.9, 4.0±1.5, 14.2±1.8, 867.3±240.5, 8.1±0.5, 58.9±0.5, 15.2±3.2, 4.2±0.7); CAG with symptoms group (2.0±1.8, 3.4±1.5, 13.4±1.8, 800.9±221.8, 8.6±0.4, 59.3±0.5, 16.5±3.1, 4.5±0.6). The contents of Zn, Cu in mitochondria and SOD in gastric mucosa of each group were shown as follows: Normal control group (9.2±0.5, 58.3±0.3, 170.5±6.1), CSG without symptoms group (8.9±0.5, 58.2±0.3, 167.2±5.3), CAG without symptoms group (8.8±0.4, 57.5±0.2, 166.1±4.2); F type with symptoms group (8.9±0.5, 58.0±0.3, 167.9±5.7), CSG with symptoms group (8.6±0.5, 57.8±0.3, 163.3±5.6); CAG with symptoms group (8.3±0.4, 57.5±0.3, 161.2±4.3). There were significant differences in these cases, $P < 0.05-0.001$. There were synchronous changes of gastric mucosa epithelial cellular ultrastructure. The "background lesions" (focal atrophic gastritis, focal intestinal metaplasia, micro-ulcer) in nonfocal gastric mucosa of all groups had significant differences ($P < 0.05-0.001$).

CONCLUSION: Disease with symptoms, disease without symptoms, nondisease with symptoms occur on the basis

of the quantitative changes of gastric mucosa epithelial cellular ultrastructure and related bioactive substances.

Yin GY, Zhang WN, He XF, Chen Y, Shen XJ. Study on the classification of chronic gastritis at molecular biological level. *World J Gastroenterol* 2003; 9(4): 836-842

<http://www.wjgnet.com/1007-9327/9/836.htm>

INTRODUCTION

After undergoing gastroscopy with mucosal biopsy, patients with digestive tract symptoms and volunteer blood donors without any clinical symptoms were found to be of two types: those with gastric mucosa pathological changes, and others without evident pathology. In order to explore the pathophysiological basis, we detected synchronously the epithelial cell ultrastructure, trace element, cAMP, DNA, gastric mucosa SOD, serum LPO and ³H-TdRLCT by means of histopathology, SEM, TEM with EDAX, image analysis technique, RIA and chemiluminescence method. The results were reported as follows.

MATERIALS AND METHODS

Materials

188 patients with digestive tract symptoms, had been ruled out from organic lesions of heart, lung, liver, gallbladder, pancreas, kidney or intestine by physical examination, fluoroscopy of chest, GI x-ray examination, type ultrasonography, blood biochemistry, gastroscopy with histopathological examination. According to diagnostic criteria of "the standards for the classification of chronic gastritis, gastroscopy atrophic gastritis", 68 cases were diagnosed as CSG (43 males, 25 females, average age 43, average course of disease 4a); 64 cases as CAG (37 males, 27 females, average age 47, average course of disease 6a.); 56 cases as having basically normal gastric mucosa (F group) (22 males, 34 females, average age 39, average course of disease 2a). Among 42 volunteer blood donors without any clinical symptoms, through gastroscopy and histopathological biopsy, 18 cases were diagnosed as CSG (13 males, 5 females, average age 39), 9 cases as CAG (7 males, 2 females, average age 41); 15 cases as having basically normal gastric mucosa (6 males, 9 females, average age 37) thus also referred to as normal control group (NC group).

Methods

During gastroscopy, three pieces of gastric mucosa were taken from the focal, nonfocal areas of antral region of stomach and body of stomach for histopathological examination, SEM, TEM, the determination of cAMP and SOD. Blood specimens were taken to determine LPO and ³H-TdRLCT. For the study of gastric mucosa ultrastructure and determination of its trace elements, 501B SEM with 9100/60 EDAX were used taking three pieces of specimens from each patient and determine the weight percentage (WT%)^[1-4] of each element between the elements of gastric mucosa. Radioimmuno-assay was adopted

to detect gastric mucosa cAMP content (pmol/g)^[5], blood ³H-TdRLCT (Bq/L)^[5]. For the observation of gastric mucosa epithelial cellular ultrastructure and the determination of its trace elements, EM 430 TEM with 9100/60 EDAX^[1-4] were used. The three pieces of mucosa specimens of every patient were magnified in unison by five magnifying powers (3 600, 7 200, 14 000, 19 000, 29 000) to randomly take pictures of the panoragram, local area and organelle and to determine the atomic number percentage (AT %) of each nuclear and mitochondrial element between the trace elements. 50 nuclei and 50 mitochondria of each patient were determined, with average WT% of each element taken as its actual WT%. For the determination of DNA in gastric mucosa epithelial nuclei, IBAS 2000 image analysis technique was used to determine IOD with gastric mucosa cell smear after Feulgen staining, taken as the relative content of nuclear DNA^[4]. Chemiluminescence method was adopted to determine the activity of SOD (u/g) in gastric mucosa^[5]. Thiobarbituric acid development process was adopted to determine serum LPO (umol/L)^[5].

Statistical method

χ^2 and *t* test.

RESULTS

Histopathological changes of gastric mucosa

In NC group and F group, there were extremely small number of mononuclear cells and lymphocytes in lamina propria of gastric mucosa, there was no abnormality in gastric gland. Therefore their gastric mucosa were defined as relatively normal. In CG gastric mucosa, in there were various degrees of infiltration of lymphocyte, plasmocyte, eosinophil and neutrophil in lamina propria, there were various degrees of degeneration necrosis, erosion and atrophy in mucosa epithelial cells. Glands decreased due to destruction and some glands had cystic dilatation. As for the inflammatory cell infiltration degree in gastric mucosa and the decrease degree of original glands (<1/3 low-grade, >1/3 <2/3 middle-degree, >2/3 heavy-grade). There was greater significant difference in CSG without symptom (CSG-woS) group, CAG without symptom (CAG-woS) group, CSG with symptom (CSG-wS) group, CAG with symptom (CAG-wS) group than in HC group and F group ($P<0.05-0.001$). There was significant difference between the first four groups ($P<0.05-0.001$, Table 1).

Ultrastructure of gastric mucosa

The relatively normal gastric mucosa had clear surface, which was divided by crisscross small groves into many lesser gastric areas, assuming convolution shape, in which there were many gastric pits (the mouths of gastric glands). The gastric pits were shaped like craters and their concave walls had round or oval epithelial cells of almost the same size (Figure 1). When magnified, the surfaces of cells were found to be rough and uneven, with short and thin microvilli as well as many semicircular cumuli, several micro processus and small fossae. The fossae were marks left by cumuli after rupture and excretion of mucus. The crater periphery projections were shaped like dykes. The gastric antrum mucosa were rough, apparently folded, the small craters were mostly groves of different lengths with deep bottoms. In low power observation, as far as gastric mucosa of chronic gastritis was concerned, the crisscross groves of the focal mucosa are shallow, the convolution structures were smooth and even, craters were deformed and of different sizes at different heights and ill-distributed; the dykes form projections that are undulating, of different width (Figure 2).

In high power observation, the focal gastric mucosa had scattering denatured, diabrotic and necrotic exfoliated epithelial cells, on it's surfaces S-shape helicobacter pylori were found (Figure 3). Massive epithelial cells were diabrotic, anabrotic and exfoliated forming micro ulcers. The ulcers spread from their centers, with adjacent cells crushed and destructed, in irregular shapes and arrangement. The epithelial cells of the crater walls were atrophic and denatured of different sizes and derangement (Figure 5), and the cells became diabrotic and necrotic and had inflammatory cell infiltration (Figure 6). The glands propria of the serious cases were shaped like grid framework structure (Figure 7). The surfaces of the epithelial cells of IM gastric mucosa were covered with a thick coating, villi were invisible, and the intercellular boundaries were not clear (Figure 8). The hollowed crateriform cells were round or polygon cavities, with ejected mucus at mouths scattering like tiny white dots. In nonfocal gastric mucosa, focal atrophic inflammatory changes, IM cell population, micro ulcers and helicobacter pylori (can be found also), they were generally referred to as "background lesion".

Comparing CSG-woS group, CAG-woS group, CSG-wS group and CAG-wS group, there were significant differences in background lesion of nonfocal gastric antrum mucosa ($P<0.05-0.001$). The incidence rate of background lesion of nonfocal gastric mucosa is especially high in CAG-wS group (Table 2).

The ultrastructure of gastric mucosa epithelial cells

The mucous cells on epithelial cell surface of relatively normal gastric mucosa were columnar epithelial cells covering endogastric surfaces and inside wall of gastric pits. Their free surfaces had short microvilli and nuclei were relatively big, at the bottoms of the cells. In cytoplasm were mucous granules of various sizes, a great deal of RERs and scattered mitochondria. The mucous neck cells were distributed over the necks of gastric glands, round or crescent shape. In the upper part of cytoplasmic nuclei, there were a great deal of secretory granules, developed Golgi's bodies, a few RERs and scattered mitochondria. On the tops of cells were a few short thick micro villi. Chief cells were distributed over the bodies and bottoms of gastric glands and their nuclei were round. In cytoplasm there are many parallel RERs, a great deal of secretory granules, well-developed Golgi's bodies and scattered mitochondria (Figure 9). The parietal cells were big and conic in shape and their conical tops turned towards gland cavities. The nuclei were in the centers of the cells. The cytosols are filled with vesicular smooth RERs (secreting hydrochloric acid), intracellular canaliculi (conveying hydrochloric acid) and many mitochondria. The endocrine cells lay between chief cells and parietal cells. They were small and their nuclei are round, at the bottoms of cellular matrixes. In cytoplasm, there are great deal of spherical endocrine granules, RERs, and a few mitochondria, Golgi's bodies lie nearby nuclei (Figure 10). The normal gastric mucosa epithelial cell nuclei were round or oval; the nuclei envelopes are slightly bending; lobulated nuclei were few; the nucleocytoplasmic ratio was less than 1; the nuclei chromatins were scattered, associated with nucleoli or distributed around the nuclei. The light bright zones between heterochromatins in the nucleoli were euchromatins; the nucleoli had high electron density without capsules (Figure 11). The normal epithelial cell mitochondria of gastric mucosa were round or oval, scattered around nuclei. The mitochondria consist of outer membrane, inner membrane, outer ventricle, inner ventricle and cristae. Crista, the inward folded inner membrane, was a hollow canal leading to outer ventricle. Some mitochondrial cristae lead directly to

cytoplasm. Cristas were generally in tabular arrangement, parallel to each other and vertical to mitochondrial long axes (Figure 12). The free surfaces of epithelial cells of CG gastric mucosa have dropped off micro villi. The intercellular space expands and cell junctions decrease; mitochondria decrease, become swollen or cristae break and had vacuolar degeneration (Figure 13). RERs dilate and were in circular arrangement. The Golgi's bodies became atrophic and had lost their typical structures; the cytoplasmic secretory granules decreased; nuclei expand or shrink; parietal cell intracytoplasmic canaliculi dilate and micro villi become short and thin or even disappear. The karyoplasmic ratio of the cells with undifferentiated nuclei and IM cells of CG gastric mucosa epithelial cells were greater than 1 and there is increase in nuclear lobulation (Figure 14), interchromatic granules, perichromatic granular density and euchromatins. The nucleoli were hypertrophic and lie close to nuclear margins (referred to as nucleolar margination). The obsolescent epithelial nuclei shrink and the nucleocyto-plasmic ratio was still less. The heterochromatins lie densely around nuclei; the electron density was low in the center of nuclei and nuclei were loop in shape (referred to as chromatic margination) (Figure 15). The shrunken nuclei were denticular, in which the electron density was moderately homogeneous and chromatin were not found (referred to as chromatic homogenization). As for the above changes, there was significant difference between NC group, CSG-woS group, CAG-woS group, F-wS group, CSG-wS group and CAG-wS group ($P < 0.05-0.001$, Table 3). There were mitochondrial swelling, hypertrophy, pyknosis, hyaline degeneration as well as vacuolar degeneration in epithelial cells of CG gastric mucosa.

Deformed mitochondria were in C-shape or U-shape. There were zigzag, longitudinal, sparse, pyknosis and deranged cristae (Figure 16). There was an decrease in the number of mitochondria and their cristae. In the above changes, there is significant difference between NC group, CSG-woS group, CAG-woS group, F-wS group, CSG-wS group and CAG-wS group ($P < 0.05-0.001$, Table 4).

Gastric mucosa trace elements, cAMP, SOD and blood $^3\text{H-TdRLCT}$

Under the direct vision of SEM with EDAX probe that automatically detected the samples within 0.1-0.01 mm² range all the elements under 12 in atomic number and automatically calculates the weight percentage (WT%) of each element in the element series. 15 points were fixed in the three pieces of mucosa from every patient to carry out 15 detections and in every detection, 21 elements were detected to get their respective average WT% as its actual WT%. Zn and Cu were taken as index. The gastric mucosa Zn, Cu, cAMP, SOD and $^3\text{H-TdRLCT}$ decrease progressively in the sequence of NC group, CSG-woS group, CAG-woS group, F-wS group, CSG-wS group and CAG-wS group ($P < 0.05-0.001$, Table 5).

Biochemical changes in gastric mucosa and blood serum

The quantity of nuclei DNA, Zn, Cu and serum LPO increased progressively in the sequence of NC group, CSG-woS group, CAG-woS group, F-wS group, CSG-wS group, CAG-wS group. While mitochondrial Zn, Cu, decreased progressively in the same sequence and there were significant differences between these groups ($P < 0.05-0.001$, Table 6).

Table 1 Degree of inflammatory cell infiltration compared with the degree of decrease of original glands in gastric mucosa $n(\%)$

Group	n	Degree of inflammatory cell infiltration			Degree decrease of glands propria		
		<1/3	>1/3<2/3	>2/3	<1/3	1/3<2/3	>2/3
NC	15						
CSG-woS	18	11(61.1)	6(33.3)	1(5.6)	1(5.6)		
CAG-woS	9	5(55.6)	3(33.3)	1(11.1)	5(55.6) ^d	3(33.3)	
F-TwS	56						
CSG-wS	68	26(38.2) ^c	32(47.1)	10(14.7)			
CAG-Ws	64	19(29.7) ^{df}	21(32.8)	24(37.5) ^{df}	23(35.9) ^d	23(35.9)	18(28.1)

Compared with NC group. ^a $P < 0.05$, ^b $P < 0.01$; compared with CSG-woS group. ^c $P < 0.05$, ^d $P < 0.01$; compared with CAG-woS group. ^e $P < 0.05$, ^f $P < 0.01$, Compared with F-wS group, ^g $P < 0.05$, ^h $P < 0.01$, Compared with CSG-wS group, ⁱ $P < 0.05$, ^j $P < 0.01$, In table 2-6, the marks are the same as here.

Table 2 Focal background lesions in non-focal site of gastric mucosa $n(\%)$

Focal lesions	CSG-woS ($n=18$)		CAG-woS ($n=9$)		CSG-wS ($n=68$)		CAG-Ws ($n=64$)	
	Gastric antrum	Gastric body	Gastric antrum	Gastric body	Gastric antrum	Gastric body	Gastric antrum	Gastric body
Atrophic	1 (5.6)	0 (0.0)	1 (11.1) ^a	0 (0.0)	21 (30.9) ^{bd}	11 (16.2)	47 (73.4) ^{bdj}	27 (42.2) ^j
inflammatory lesion								
IM	4 (22.2)	1 (5.6)	5 (55.6) ^b	2 (22.2) ^b	27 (39.7) ^{bc}	5 (7.4) ^d	59 (92.2) ^{bdj}	13 (20.3) ^b
Micro ulcer	1 (5.6)	1 (5.6)	3 (33.3) ^b	1 (11.1) ^a	11 (16.2)	2 (2.9) ^c	28 (43.8) ^{bdj}	9 (14.1) ^{aj}

Table 3 Ultrastructures of gastric mucosa epithelial cell nuclei *n* (%)

Group	<i>n</i>	Appearance		Chromatin		Nucleoli	
		nucleoplasmic ratio >1	nuclear lobulation	margination or homogeneity	perinuclear concentration	hypertrophy or margination	looping
NC	15			1 (6.7)	1 (6.7)		
CSG-woS	18	1 (5.6)		4 (22.2) ^b	1 (5.6)	1 (5.6)	1 (5.6)
CAG-woS	9	2(22.2) ^d	2(22.2)	7 (77.8) ^{bd}	3 (33.3) ^{bd}	2 (22.2) ^d	4 (44.4) ^d
F-TwS	56			3 (5.4) ^{df}	3 (5.4) ^f	1 (1.8) ^f	
CSG-wS	68	5 (5.7) ^f	2(2.9) ^f	7 (10.3) ^{cf}	5 (7.4) ^f	2 (2.9) ^f	2 (2.9) ^f
CAG-Ws	64	20(31.3) ^{dj}	9(29.7) ^j	33 (51.6) ^{bdhj}	29 (45.3) ^{dffhj}	27 (42.2) ^{dffhj}	14 (21.9) ^{dgi}

Table 4 Mitochondria ultrastructures of gastric mucosa epithelial cells. ($\bar{x}\pm s$)

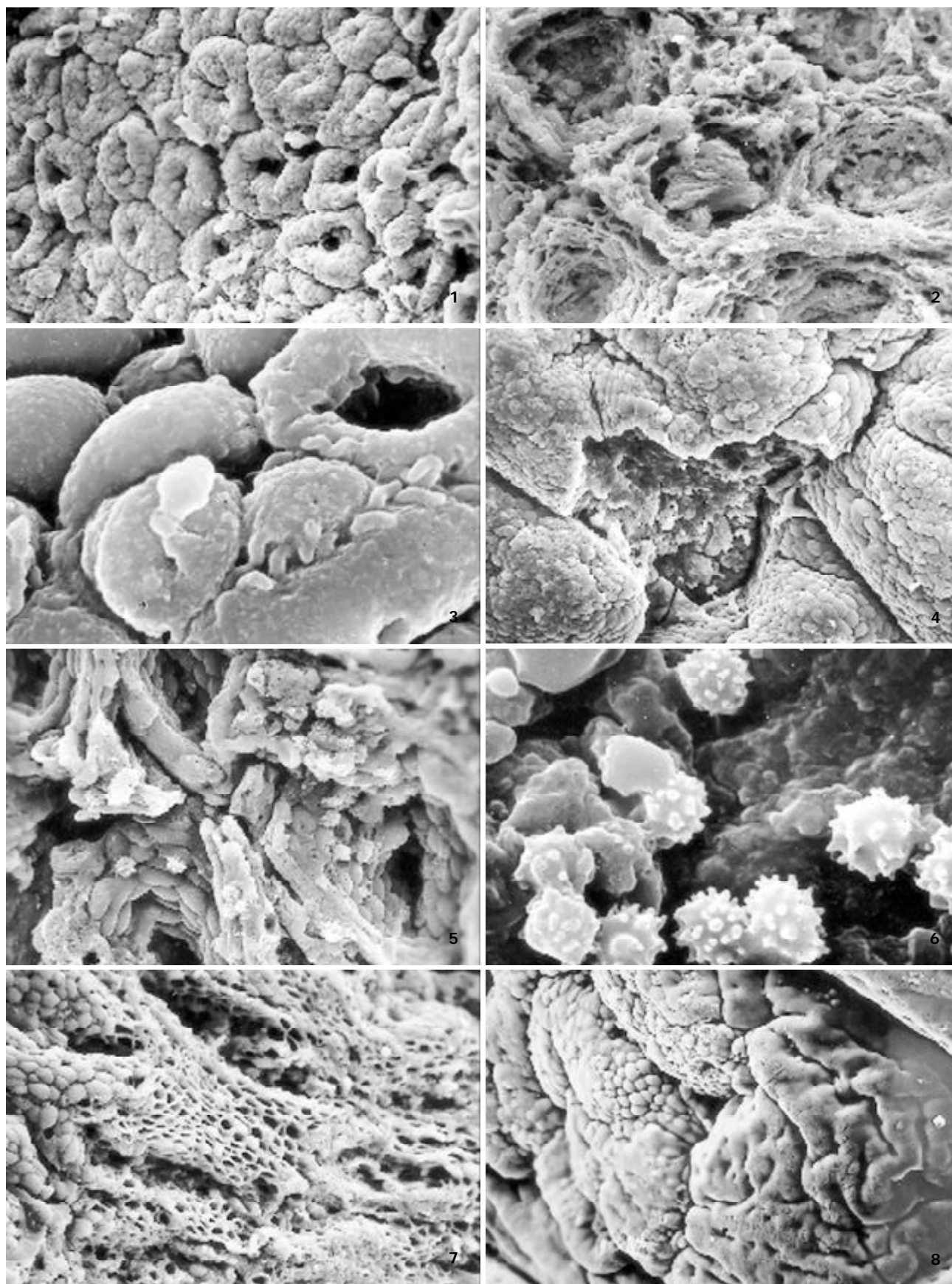
Group	<i>n</i>	Number	Swelling & overgrowth (%)	Matrix-discoloration (%)	Vacuolar degeneration (%)	Pyknosis (%)	Crista number	Crista fragmentation & derangement (%)
NC	15	86.5±27.3	3.4±1.6	3.0±1.1	2.9±1.9	1.1±0.8	12.8±3.2	2.2±1.1
CSG-woS	18	85.3±22.2	3.9±1.1	3.9±2.2	3.2±1.2	1.4±0.9	11.4±2.4	3.1±1.3
CAG-woS	9	83.8±17.3	4.4±2.4	4.3±2.9	3.3±1.1	1.7±0.8	11.4±2.1	3.2±1.2
F-TwS	56	83.1±22.8	5.4±2.9 ^{bd}	4.4±2.4	2.9±1.8	1.2±0.7	11.2±2.3	3.9±1.2 ^{bc}
CSG-wS	68	65.4±21.1 ^{bdfh}	7.2±3.8 ^{bdfig}	7.9±5.0 ^{bdfh}	6.4±4.5 ^{bdfh}	1.9±0.9 ^{bch}	8.2±3.2 ^{bdfh}	5.8±3.1 ^{bdfh}
CAG-wS	64	52.2±20.8 ^{bdfhj}	10.9±4.5 ^{bdfhj}	11.7±8.6 ^{bdfhj}	11.6±7.7 ^{bdfhj}	3.7±1.1 ^{bdfhj}	6.9±3.5 ^{bdfhji}	8.9±3.7 ^{bdfhj}

Table 5 Gastric mucosa trace elements, cAMP and ³H-TdRLCT ($\bar{x}\pm s$)

Group	<i>n</i>	Gastric mucosa				Blood
		Zn (WT%)	Cu (WT%)	cAMP (Pmol/g)	SOD (u/g)	³ H-TdRLCT (Bq/L)
NC	15	4.1±1.0	5.2±0.8	15.9±1.5	170.5±6.1	1079.7±227.4
CSG-woS	18	3.7±1.2	5.1±1.8	15.6±0.9	167.2±5.3	924.5±234.9
CAG-woS	9	3.3±1.0	4.8±0.9	14.9±0.7 ^a	166.1±4.2 ^a	887.7±243.6
F-TwS	56	3.5±1.4 ^a	4.5±1.0 ^a	15.7±1.4 ^e	167.9±5.7	932.1±2449.3 ^a
CSG-wS	68	2.8±1.9 ^{bcg}	4.0±1.5 ^{aceg}	14.2±1.8 ^{bdeh}	163.3±5.6 ^{bdh}	867.3±240.5 ^{bc}
CAG-wS	64	2.0±1.8 ^{bdfhi}	3.4±1.5 ^{bdfhj}	13.4±1.8 ^{bdfhi}	161.2±4.3 ^{bdfhi}	800.9±221.8 ^{bdi}

Table 6 Epithelial nuclei and mitochondria Zn, Cu in gastric mucosa ($\bar{x}\pm s$)

Group	<i>n</i>	Nuclei			Mitochondria		Serum
		Zn (AT%)	Cu(AT%)	DNA(IOD)	Zn (AT%)	Cu(AT%)	LPO(umol/L)
NC	15	7.6±0.4	58.4±0.3	12.6±2.7	9.2±0.5	58.3±0.3	2.6±0.6
CSG-woS	18	7.8±0.3	58.6±0.4	13.0±3.1	8.9±0.5	58.2±0.3	2.9±0.4
CAG-woS	9	7.8±0.3 ^a	58.7±0.3 ^a	14.3±2.8	8.8±0.4 ^a	57.5±0.2 ^{bd}	3.1±0.4
F-TwS	56	7.9±0.4 ^a	58.7±0.5 ^a	13.5±4.6	8.9±0.5 ^a	58.0±0.3 ^{af}	2.9±0.7
CSG-wS	68	8.1±0.5 ^{bdfh}	58.9±0.5 ^{bdh}	15.2±3.2 ^{bcg}	8.6±0.5 ^{bh}	57.8±0.3 ^{bdfh}	4.2±0.7 ^{bdfh}
CAG-Ws	64	8.6±0.4 ^{bdfhj}	59.3±0.5 ^{bdfhj}	16.5±3.1 ^{bdehi}	8.3±0.4 ^{bdfhj}	57.5±0.3 ^{bdfhj}	4.5±0.6 ^{bdfhi}



- Figure 1** Mouth of gastric glands, like craters, The concave walls have round or oval epithelial cells, of almost same size. $\times 160$.
- Figure 2** Craters are deformed, the crater periphery projections are of different heights and width. $\times 320$.
- Figure 3** On cell surfaces, S-shape *Helicobacter pylori* are found. $\times 2\ 500$.
- Figure 4** Micro ulcers. $\times 320$.
- Figure 5** Epithelial cells of crater concave walls are atrophic, denatured, of different sizes and deranged. $\times 640$.
- Figure 6** Inflammatory cell infiltration. $\times 2\ 500$.
- Figure 7** Glands propria of grid framework structure. $\times 320$.
- Figure 8** Surface of IM gastric mucosa epithelium is thickly coated, villi are invisible, intercellular boundaries are not clear. $\times 320$.

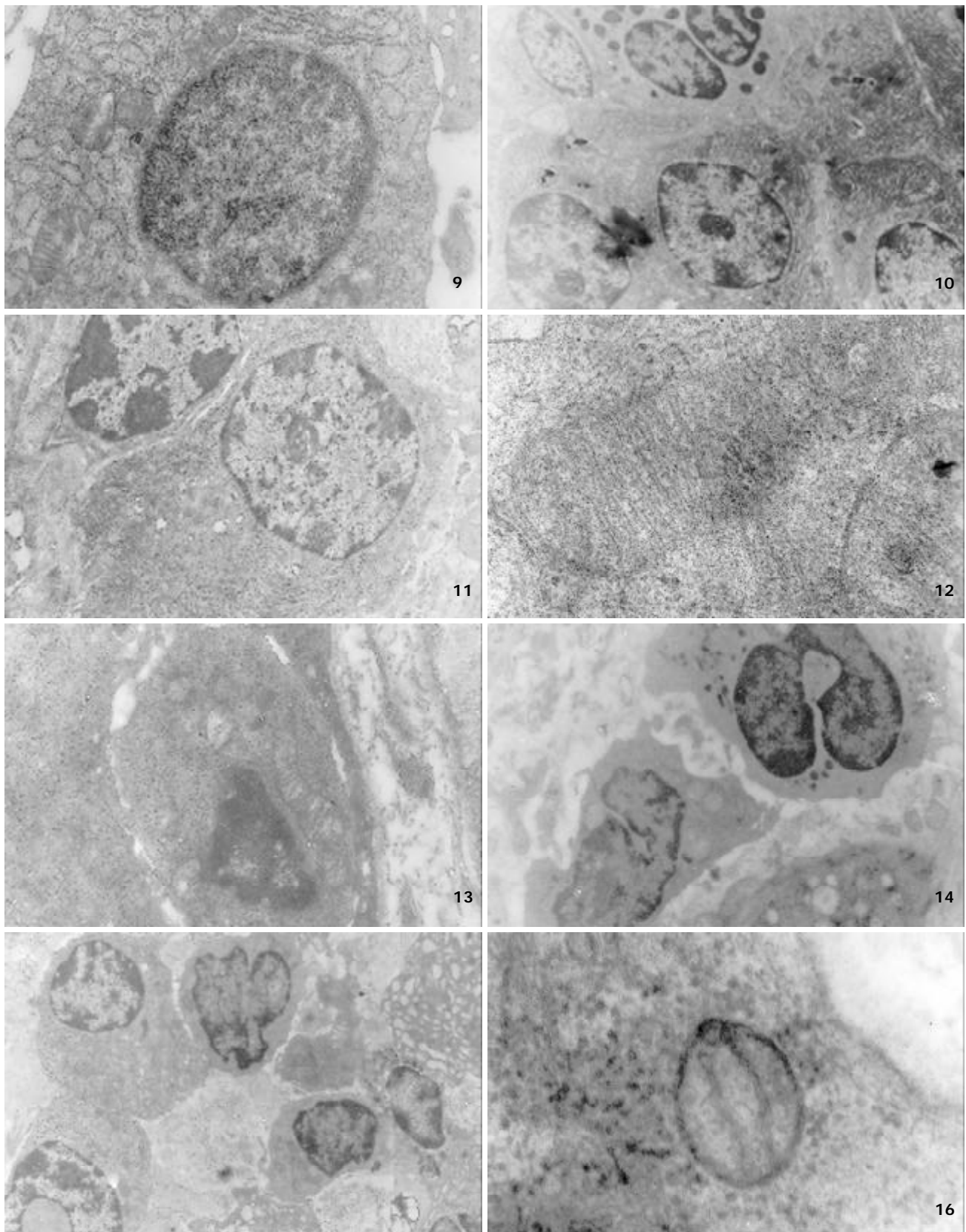


Figure 9 Normal epithelial nuclei are round, there are RERS, secretory granules, Golgi's bodies and mitochondrias in cytoplasm. $\times 7\ 200$.

Figure 10 The normal epithelial secretory cells are relatively small, nuclei are round, a great deal of spherical incretory granules in cytoplasm. $\times 14\ 000$.

Figure 11 Normal gastric mucosa epithelial nuclei are round. or oval, nucleocytoplasmic ratio <1 ; the nucleoli have no capsules. $\times 14\ 000$.

Figure 12 Normal cristas are hollow canals leading to outer ventricles. cristas are vertical to mitochondrial long axles. $\times 14\ 000$.

Figure 13 Intercellular space expands, decrease of cellular conjunctions; mitochondria decrease, swollen or cristae break, have vacuolar degeneration. $\times 29\ 000$.

Figure 14 Nucleocytoplasmic ratio >1 , lobulated nuclei. $\times 7\ 200$.

Figure 15 Heterochromatins lie densely around nuclei, the electron density is low in the centers of nuclei. the nuclei are loop in shape (referred to as chromatic homogenization). $\times 14\ 000$.

Figure 16 Longitudinal cristas, sparse cristae, deranged cristae. $\times 14\ 000$.

DISCUSSION

Compared with NC group, 188 patients with digestive tract symptoms without other organic disease and 27 patients without any clinical symptoms have a tendency of decreasing of quality in the submicrostructure of gastric mucosa epithelial cells -mitochondria. The incidence rate of karyoplasmic ratio > 1, nuclear lobulation, chromatin peripheral granule densification, hypertrophy of nucleoli, mitochondrial degeneration, and quantitative changes of nucleolar DNA, Zn, Cu and LPO increase progressively in the sequence of NC group, CSG-woS group, CAG-woS group, F-wS group, CSG-wS group and CAG-wS group. While gastric mucosa Zn, Cu, cAMP, SOD and mitochondrial Zn, Cu and the number of mitochondria and crista decrease progressively in the same sequence.

When gastric mucosa is damaged by noxious substances or ischemia, the metabolism of Zn, Cu becomes disordered with the body and thus enzyme system is disturbed. In human body, Zn is the important component and activator of over a hundred varieties of enzymes such as carbonic anhydrase, DNA polymerase, peptase, phosphatase, peroxide dismutase etc. By regulating the activity of these enzymes, it participates and regulates the metabolism of sugars, lipids, proteins, nuclei acid and vitamins, contends for mercaptan to inhibit free radical reaction. Cu participates the composition of over 30 kinds of proteins and enzymes in the body, regulates the protein metabolism and influences cellular respiration and division. When the level of Zn and Cu in the body declines, the synthesis and activity of SOD will be inhibited. Because of NADPH oxidation reduction circulation and the catalytic function of xanthine oxidase, a great deal of oxygen free radicals will be produced, far beyond the clearing ability of SOD. The excessive accumulated oxygen free radicals react in peroxidation with unsaturated fatty acid of inner and outer mitochondrial membranes and produce LPO, therefore serum LPO level will rise. The inner and outer mitochondrial membranes will accordingly be damaged, resulting in the decrease and derangement of mitochondrial cristae, the change of the ratio of mitochondrial ventricle diameter to cavity diameter and eventually the retrograde affection, the decrease of ATP production, inadequate energy supply, which in turn cause debility, structural atrophy, decrease of gastric acid secretion and even cytonecrosis. The participation of Zn and Cu dependence enzymes is essential in nuclear protein synthetic metabolism (including DNA duplication) and mitochondrial energy metabolism. When nuclear took in more Zn and Cu, the protein synthesis was brisk, nuclei division and hyperplasia were accelerated, which increased the chance of gene mutation. As the second messenger substance, cAMP regulate some vital activities in the body. Once the quantity of cyclic nucleoside phosphate in nuclei changes abnormally, pathological state will occur. The quantitative changes of cAMP result in the changes of cellular metabolism, immunity and vegetative functions. The decrease of cyclic nucleoside phosphate, especially cAMP in the body results in the inhibition of sympathetic nerve (including purinergic nerve) function, and relative hyperfunction of parasympathetic nerve function. As a result, digestive tract symptoms occur such as abdominal distention, loose stool, involuntary drooling, poor appetite, pale enlarged tongue with tooth marks. Through influencing lymphocyte metabolism, the quantitative changes of Zn and cAMP in turn influence cell respiration, differentiation and inhibit lymphocyte transformation^[4,6-13] and cause decline of ³H-TdRLCT level. As a result: (1) When gastric mucosa Zn, Cu and blood ³H-TdRLCT are nearly equal to that of NC group and gastric mucosa cAMP was markedly lower than that of

HC group, clinical phenomena as CSG-woS and CAG-woS will occur; (2) When gastric mucosa Zn, Cu and ³H-TdRLCT were markedly lower than that of NC group and gastric mucosa cAMP is nearly equal to that of NC group, the phenomenon of F type with symptoms (non-disease with symptoms) will occur; (3) When the levels of gastric mucosa Zn, Cu, cAMP and ³H-TdRLCT were all markedly lower than those of NC group, the clinical phenomena such as CSG-wS and CAG-wS will occur. The occurrences of these clinical phenomena were consistent with the change of gastric mucosa ultrastructure and histopathology, forming the pathophysiological basis in the classification of chronic gastritis. Thus it can be seen that changes of gastric mucosa epithelial cell ultrastructures and the quantitative changes of their bioactive substances are the pathophysiological bases that determines the classification of chronic gastritis with different classification has respective clinical symptoms.

REFERENCES

- 1 **Yin GY**, Zhang WN, He XF, Chen Y, Shen XJ. Detection of ultrastructural changes and contents DNA, Zn, Cu and LPO in subgroups of chronic gastritis. *Shijie Huaren Xiaohua Zazhi* 2002; **10**: 663-667
- 2 **Yin GY**, Zhang WN, Shen XJ, Chen Y, He XF. Ultrastructural and molecular biological changes of chronic gastritis and gastric cancer: a comparative study. *Shijie Huaren Xiaohua Zazhi* 2002; **10**: 668-672
- 3 **Yin GY**, Zhang WN, He XF, Chen Y, Shen XJ. Alterations of ultrastructures, trace elements, cAMP and cytoimmunity in subgroups of chronic gastritis. *Shijie Huaren Xiaohua Zazhi* 2002; **10**: 673-676
- 4 **Yin GY**, Zhang WN, He XF, Chen Y, Yin YF, Shen XJ. Histocytological study on gastric mucosa of spleen deficiency syndromes. *Zhongguo Zhongxiyi Jiehe Zazhi* 1999; **19**: 660-663
- 5 **Yin GY**, Xu FC, Zhang WN, Li GC, He XF, Chen Y, Shen XJ. The effect of weikangfu on cytopathology of gastric mucosa tissue when treating gastric precancerous lesion of patients with spleen deficiency syndromes. *Zhongguo Zhongxiyi Jiehe Zazhi* 2000; **6**: 241-243
- 6 **Yin GY**, Zhang WN, Xu FC, He XF, Chen Y, Shen XJ. Effect of Weikangfu chongji on ultrastructure of precancerous gastric mucosa of patients with spleen deficiency Syndromes. *Zhongguo Zhongxiyi Jiehe Zazhi* 2000; **20**: 667-670
- 7 **Yin GY**, Zhang WN, Xu FC, Chen Y, He XF, Li GC, Shen XJ. Study on the modern pathophysiologic basis of the syndrome classification of spleen deficiency with chronic gastritis and of (treatment) verification of clinical syndromes and prescriptions. *Jiangsu Yiyao Zazhi* 2001; **27**: 46-47
- 8 **Yin GY**, He XF, Yin YF, Du YQ, Jiao JH. Study on mitochondrial ultrastructure, trace elements and correlative factors of gastric mucosa in patients with spleen deficiency syndrome. *Zhongguo Zhongxiyi Jiehe Zazhi* 1996; **15**: 719-723
- 9 **Yin GY**, Zhang WN, Xu FC, He XF, Chen Y, Shen XJ. Effect of weikangfu chongji on epithelial cellular ultrastructure of precancerous gastric mucosa of patients with spleen deficiency syndrome. *Jiangsu Yiyao Zazhi* 2000; **26**: 514-517
- 10 **Yin GY**, Zhang WN, Xu FC, He XF, Chen Y, Li GC, Shen XJ. Effect of weikangfu on Zn, Cu and DNA in precancerous gastric mucosa epithelial nuclei and mitochondria of patients with spleen deficiency syndromes. *Zhongguo Zhongxiyi Jiehe Zazhi* 2000; **8**: 221-224
- 11 **Yin GY**, Zhang WN, Shen XJ, Chen Y, He XF. A comparative study on ultrastructure of chronic gastritis gastric mucosa IM, ATP and their molecular biology. *Jiangsu Yiyao Zazhi* 2002; **28**: 4-7
- 12 **Yin GY**, He XF, Zhang WN, Chen Y. Relationship between the classification of spleen deficiency and the quantitative changes of bio-active substances in mitochondria of gastric mucosa epithelial cell nuclei. *Zhongguo Zhongxiyi Jiehe Zazhi* 1999; **7**: 145-148
- 13 **Yin GY**, Zhang WN, Li GC, Huang JR, Chen Y, He XF, Shen XJ. Therapeutic effect of weikangfu on gastric precancerous disorder with spleen deficiency syndrome and its effect of gastric mucosal zinc, copper, cyclic adenosine monophosphate, superoxide dismutase, lipid peroxide and ³H-TdR lymphocyte conversion test. *Zhongguo Zhongxiyi Jiehe Zazhi* 2000; **20**: 176-179